Synthesis of High Quality Monolayer Graphene at Reduced Temperature on Hydrogen-Enriched Evaporated Copper (111) Films

Li Tao,[†] Jongho Lee,[†] Harry Chou,[‡] Milo Holt,[†] Rodney S. Ruoff,[‡] and Deji Akinwande[†,*]

[†]Microelectronics Research Center, Department of Electrical Engineering, [‡]Department of Mechanical Engineering and the Texas Materials Institute, The University of Texas at Austin, Austin, Texas 78758, United States

ABSTRACT

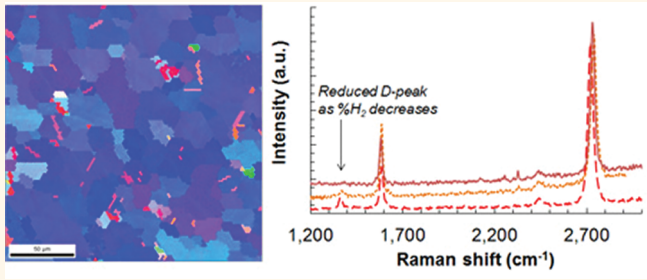

We report new findings on the chemical vapor deposition (CVD) of monolayer graphene with negligible defects (≥95% negligible defect-peak over 200 μm × 200 μm areas) on evaporated copper films. Compared to copper foils used in the CVD of graphene, several new unexpected results have been observed including high-quality monolayer synthesis at temperatures <900 °C, a new growth window using a hydrogen-free methane precursor for low-defects, and electron microscope evidence of commensurate growth of graphene grains on underlying copper grains. These thermal, chemical, and physical growth characteristics of graphene on copper films can be attributed to the distinct differences in the dominant crystal orientation of copper films (111) versus foils (100), and consequent dissimilar interplay with the precursor gas. This study suggests that reduced temperature, hydrogen-free synthesis of defect-negligible monolayer graphene is feasible, with the potential to shape and scale graphene grains by controlling the size and crystal orientation of the underlying copper grains.

KEYWORDS: graphene · chemical vapor deposition · Cu (111) · hydrogen · crystal orientation · methane

Recent progress in the synthesis of large area single and few layer graphene[1−4] has enabled study of various potential sensor, optical, thermal, and electronic applications.[5−10] The application of graphene for next generation nanoelectronics and nanotechnology, however, requires high quality films with low defect density and high uniformity. One of the most practical methods is the chemical vapor deposition (CVD) of graphene on evaporated copper film on various supporting substrates, which has the potential for direct integration into standard device manufacturing processes.[11−14] In contrast to high quality graphene grown on copper foils,[1−3] monolayer graphene grown on evaporated copper thin film has had (up until now) relatively lower quality with regards to the following metrics measured by Raman spectroscopy: (i) a wider 2D-peak or reduced 2D-peak to G-peak intensity ratio (I_{2D}/I_G) suggesting the presence of few layer films, or (ii) substantial D-peak intensity signifying appreciable defect density.[11−13,15−17] This article reports new findings in CVD graphene on evaporated copper film that show that there are noticeable differences between the evaporated copper film and the conventional copper foils in terms of the thermal, chemical, and physical growth characteristics. Electron microscope images indicate that commensurate monolayer graphene was obtained in conditions that have not been successful on copper foils (e.g., lower temperature and in a hydrogen-free methane precursor). For the thermal CVD growth of graphene on copper foils, the lowest reported temperature using methane precursor is 800−850 °C by Lee *et al.*,[16] and Cai *et al.*,[18] albeit with substantial defects or the presence of multilayers. Also, Gao *et al.*,[19] reported the ultrahigh vacuum epitaxial growth of graphene on single crystal Cu (111), but with a large defect-peak and small domains. Moreover, it has been reported by Vlassiouk *et al.*,[17] that there exists an optimum ratio of hydrogen gas to hydrocarbon gas to facilitate low-defect monolayer graphene growth on copper foils owing to the competition between growth

* Address correspondence to deji@ece.utexas.edu.

Received for review November 16, 2011 and accepted February 7, 2012.

Published online February 07, 2012
10.1021/nn205068n

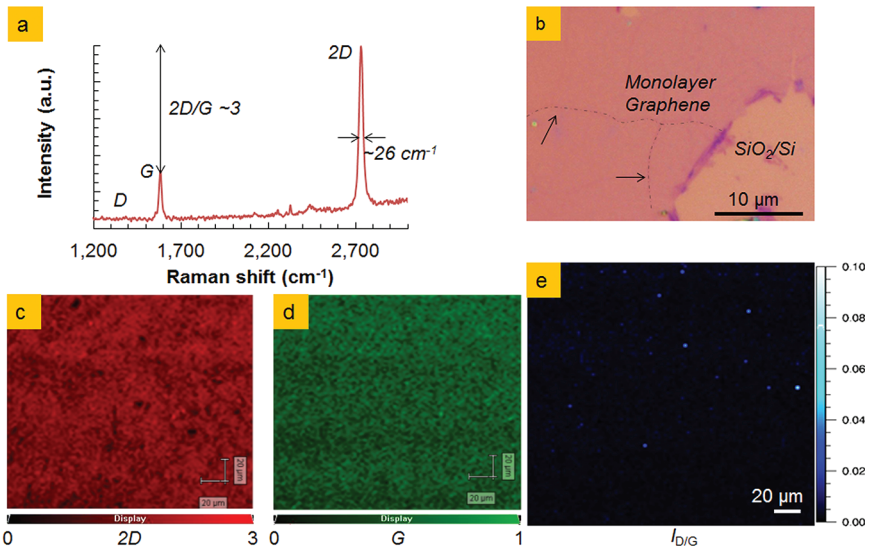

Figure 1. Low-pressure chemical vapor deposition of graphene on evaporated copper film at 975 °C: (a) Raman spectroscopy with 442 nm laser indicating defect-negligible monolayer graphene examined directly on the copper surface. The full width at half-maximum (fwhm) of the 2D-peak is ~26 cm^{-1}, I_{2D}/I_G ratio is ~3, and there is no measurable D-peak. (b) Optical image of the monolayer graphene transferred to SiO_2/Si substrate. The boundaries among graphene domains are indicated by dashed lines and arrows as a visual guide. (c–e) Raman mapping of graphene in a 200 × 200 μm^2 area, indicating the uniform intensities of the 2D-peak, G-peak, and the (negligible ratio of) D/G intensity, respectively.

and etching of graphene. In the work reported here, monolayer graphene with negligible defects was obtained for the first time on vapor-deposited Cu films on standard oxidized silicon at a temperature below 900 °C *via* thermal CVD without hydrogen gas in the growth phase. These unexpected observations result from the differences in the preferred crystal orientations of evaporated copper film versus commercial copper foil and the subsequent interactions with the carbon precursor, as observed in this study.

RESULTS AND DISCUSSION

The synthesis procedure began with the electron-beam evaporation of 0.5–1 μm copper film at 10^{-6} Torr on a silicon wafer with ~300 nm thermal oxide. CVD synthesis of graphene on deposited copper films was carried out in a vertical cold-wall chamber with separate showerhead and substrate heaters. A typical synthesis process included a hydrogen annealing step, growth step with ultrahigh purity methane only, and a two-step cooling before unloading samples from the chamber (see Materials and Methods).

Grown samples were first characterized with a Renishaw inVia Raman microscope using a 442 nm blue laser. The blue laser has the advantage of accessing graphene vibrations (Figure 1a) directly on the copper substrate (see Supporting Information Figure S1) without the strong background signal seen with the frequently used green laser. A typical Raman spectrum of graphene synthesized on an evaporated copper film is shown in Figure 1a. The width of the 2D-peak is ~26 cm^{-1}, the I_{2D}/I_G ratio is ~3, and there is no measurable D-peak indicating the successful growth of high-quality monolayer graphene on an evaporated copper film at 975 °C. Optical microscope image (Figure 1b) showed a uniform graphene film after transfer to a standard SiO_2/Si substrate (see Supporting Information Figure S2). Dash lines and arrows were added to signify the boundaries among domains. The uniformity of synthesized graphene was further confirmed with Raman mapping data of the 2D-peak and G-peak shown in Figure 1c,d. The intensity ratio map of the D/G (Figure 1e) yields no measurable D-peak (<0.1) in approximately 95% of the scanned area. Pristine monolayer graphene with negligible defect density is of great importance for device applications. For example, the sheet resistance of graphene with substantial defects can be more than 4 times higher than graphene with negligible defects (see Supporting Information Figure S3a,b), symptomatic of a lower mean free path for charge carriers. Flexible field effect transistors made from our synthesized graphene showed a peak mobility of ~4900 cm^2/V–s (see Supporting Information Figure S3c)

To elucidate the mechanisms responsible for the high-quality graphene on copper films, detailed material investigation and growth experiments proved insightful. First, at lower growth temperatures (875–900 °C), monolayer graphene with negligible defects was obtained on evaporated copper film, which has not been achieved on copper foils under the same conditions (Figure 2). With increasing copper film thickness, the minimum temperature needed to obtain monolayer graphene also rises proportionally (see Supporting Information Figure S4). Second, hydrogen is detrimental to the growth of high quality

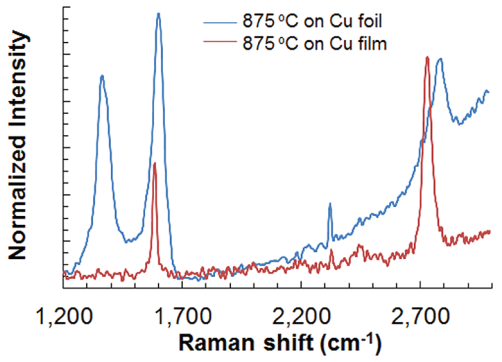

Figure 2. The effect of copper catalyst substrate on the growth of graphene. (a) Raman spectra (normalized to the 2D-peak for comparison) of graphene on 500 nm copper film and 25 μm copper foil grown at 875 °C, 10 sccm of CH_4 for 5 min. The copper film growth has clear signatures of monolayer graphene while the copper foil has strong D and G-peaks indicative of defective multilayers. Compared to high temperature (≥1000 °C) methane CVD growth on conventional copper foils, the growth of graphene can be performed at a reduced temperature, <900 °C, on evaporated copper films.

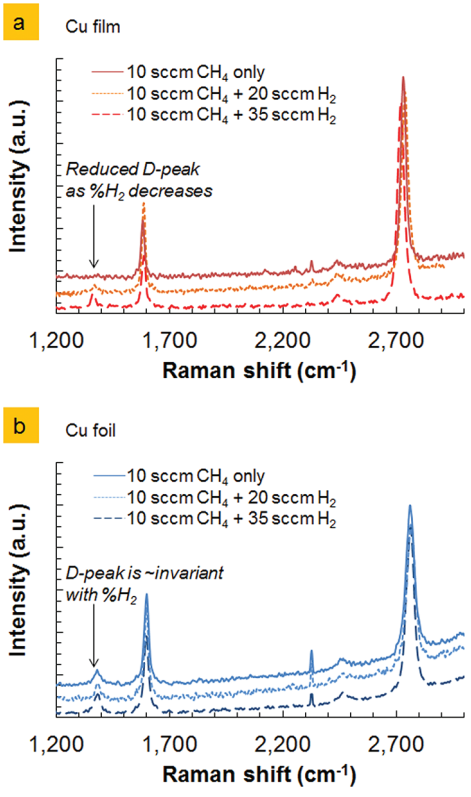

Figure 3. Stacked Raman spectra showing the effect of hydrogen on the CVD growth of graphene on (a) copper film and (b) copper foil. All growth was performed at 975 °C for 5 min, and Raman spectra were normalized to the intensity of 2D-peak before stacking for illustrative purposes. Decreasing the hydrogen ratio results in a vanishing D-peak intensity on copper films, indicating defect-negligible graphene at zero hydrogen flow. However, this trend does not apply to the copper foil substrate in the same growth conditions.

graphene on evaporated copper film, whereas it has previously been reported as a beneficial cocatalyst for

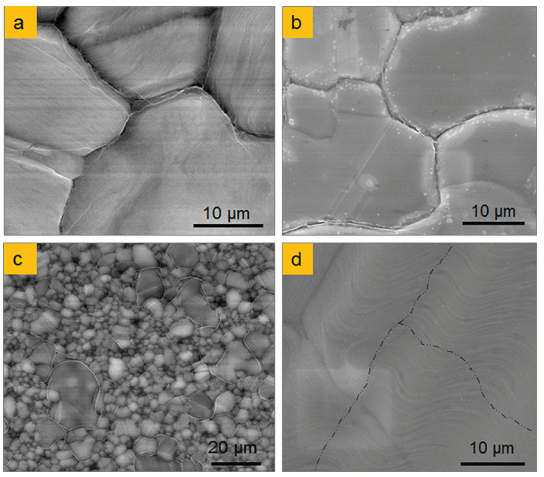

Figure 4. The correlation between graphene grains and the underlying copper grains: (a–c) Boundaries (or wrinkles) of graphene are commensurate with the grain boundaries of evaporated copper film from three separate samples. (d) Graphene domains traverse the grain boundary of copper foil (dashed lines added to illustrate the boundary of graphene domains). All samples are grown at 975 °C, 10 sccm methane with a growth time of 5 min for images a, b, and d, and 1 min for image c).

growth on copper foils.[17,20] With decreasing hydrogen to methane ratio, the D-peak of the synthesized graphene reduces and is eventually not measurable in a hydrogen-free methane environment indicating negligible defects (Figure 3a). For conventional growth on copper foils under the same conditions, a noticeable D-peak is still observed in the Raman spectrum even in the absence of hydrogen during growth (Figure 3b). In addition, the correlation between graphene and copper domains are noticeably different when comparing copper film and copper foil surfaces. The grain boundaries of the CVD graphene are commensurate with the grain boundaries of the underlying evaporated copper film (Figure 4a–c). In the case of graphene on copper foils, the graphene domains mostly traverse the grain boundaries of the underlying copper (Figure 4d) which has also been observed in other studies.[21–23] This implies a possible approach to control the size of graphene domains by controlling the size of the underlying copper grains, which is a function of process conditions including temperature and time (see Supporting Information Figure S5).

The aforementioned observation suggests a significant difference in the growth process compared to atmospheric or low-pressure CVD on copper foils.[17,24] We have performed some studies to identify and exclude some possible mechanisms behind these findings, though a complete understanding of the growth mechanism will likely require atomic resolution tools such as scanning tunneling microscopy. Additional characterization of the copper film in comparison to copper foil was performed *via* atomic force microscopy (AFM), electron back scattering diffraction (EBSD), X-ray diffraction (XRD), and time-of-flight secondary

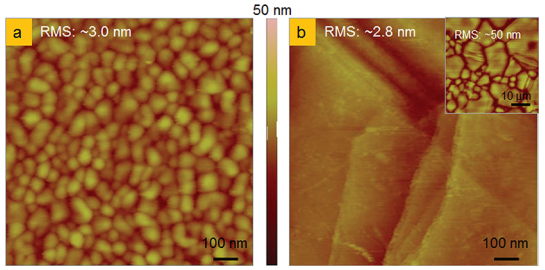

Figure 5. Surface morphology of evaporated copper film on SiO_2/Si substrates (a) before, and (b) after the CVD growth of graphene at 975 °C. Inset is a scan over a 50 × 50 μm^2 area. The rms roughness remains ~3 nm before and after the CVD process locally (1 × 1 μm^2 area), but increased to ~50 nm globally (50 × 50 μm^2 area) which is similar to the surface roughness of copper foils (typically 50−100 nm). As the images indicate, the evaporated copper film undergoes a phase transformation from "amorphous" to crystallized domains. This phase transformation plays an important role in the growth mechanism of graphene synthesis on copper films.

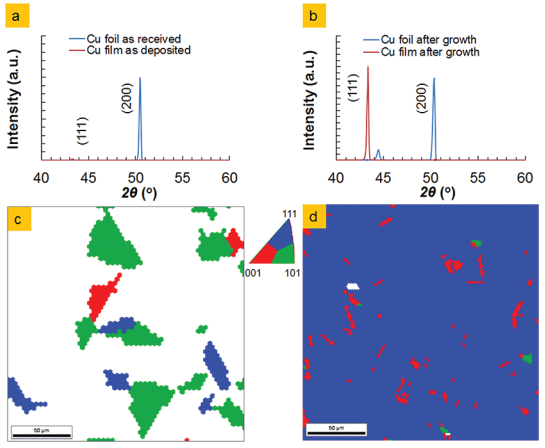

Figure 6. Crystal orientation of copper foil and evaporated copper film before and after the synthesis of graphene investigated by X-ray diffraction (XRD) and electron back scattering diffraction (EBSD). It is evident that on copper foil, the dominant orientation is (200) as indicated by $2\theta \approx 50.5°$ in the XRD spectrum. For copper film, it has undergone crystallization from (c) amorphous (white color represents no detectable orientation) to a dominant Cu (111) facet after annealing and growth as denoted at $2\theta \approx 43.3°$ in the XRD spectrum. The Cu annealing yields 96.58% (111) orientation (indicated by the area of the blue color in the EBSD map). EBSD maps were digitized into red (100), green (101), and blue (111) for better visualization. The raw data can be found in the Supporting Information Figure S6.

ion mass spectroscopy (TOF-SIMS). The first parameter investigated was the surface roughness between evaporated copper films and copper foils. Figure 5a shows that the root-mean-square (rms) roughness of as-deposited copper film is 2−3 nm. After annealing, the rms roughness of copper film is approximately 2 nm locally (1 × 1 μm^2) and 50 nm globally (50 × 50 μm^2) as shown in Figure 5b. Similar topography was observed on copper foil which has an rms roughness *ca.* 50−100 nm globally (not shown). Hence, there is no sufficient difference in the overall surface topography

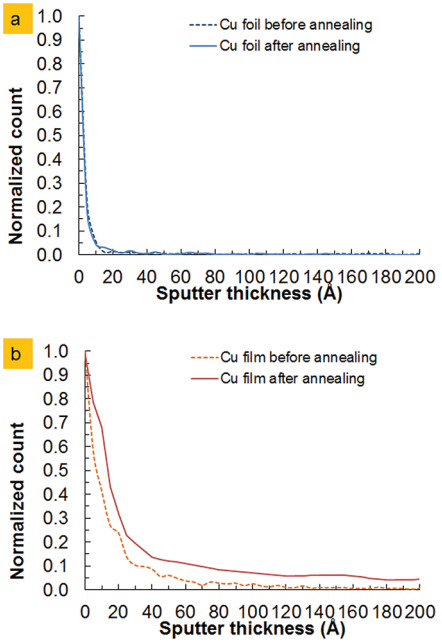

Figure 7. Time-of-flight secondary ion mass spectroscopy: depth profile of hydrogen on the surfaces of (a) copper foil and (b) evaporated copper film before and after annealing at 975 °C, 1000 sccm H_2 for 5 min. There is a noticeable increase of hydrogen content on the surface of annealed copper film, whereas no difference is observed on copper foil. This observation supports the hypothesis that absorbed hydrogen in the copper film can facilitate the decomposition of methane for the growth of high-quality graphene without the need for hydrogen gas in the methane precursor.

of copper film and foil to explain the growth findings. The second parameter studied was the grain orientation of the polycrystalline copper surface. Initially, the copper foil is polycrystalline while the evaporated copper film is mostly amorphous (Figure 6a,c). After the CVD process, the dominant facet on copper foil is (200), equivalent by translational symmetry to (100). However, for the copper film, a dominant (111) orientation is observed from both XRD (Figure 6b) and EBSD characterization (Figure 6d and Supporting Information S6). As also shown in the AFM image in Figure 5, the copper film undergoes a transformation from an "amorphous"-like film to a polycrystalline structure with the (111) hexagonal crystal orientation favoring the growth of high quality graphene.[22,23] In the CVD of graphene on copper foil, hydrogen serves as a cocatalyst and aids in the methane decomposition for the growth of graphene.[17] On the basis of published reports regarding the similarity of the adsorption kinetics of hydrogen on Cu (111) and (110) surfaces,[25,26] and their higher reactivity compared to (200) surfaces,[27] it is reasonable to expect higher hydrogen adsorption on (111) than (200) Cu facets under the same annealing condition. As a result, we surmise that a higher concentration of hydrogen is absorbed onto the Cu (111) facet during hydrogen annealing. Subsequently, this absorbed hydrogen can

TABLE 1. Comparison of the Reported Raman Signatures of CVD Synthesized Graphene on Copper Thin Film Catalyst

graphene synthesized on evaporated or sputtered copper film	$fwhm_{2D}$ (cm^{-1})	I_{2D}/I_G	I_D/I_G
this work	26–35	2–5	0–0.2
monolayers; ref 11–15	30–40	2–4	0.05–0.4
few or multiple layers; ref 13,15,16	36–40	≤2	≥0.5
mechanical exfoliation; ref 40,41	25–30	~4	~0

diffuse to the copper surface during the growth phase and promote the surface-based synthesis of monolayer graphene. The (postulated) more extensive hydrogen adsorption is supported by TOF-SIMS characterization which revealed hydrogen enriched (111) copper film compared to (200) copper foil as shown in Figure 7. For this measurement, the annealed copper foil and evaporated copper film samples were heated together in the same batch and allowed to cool down to room temperature. For the copper foil sample (Figure 7a), there was no difference in the hydrogen content on the surface before and after annealing. However, after the same annealing process, a noticeable increase in hydrogen was observed on the copper film sample (Figure 7b), which can subsequently diffuse to the surface to facilitate graphene growth on copper films, eliminating the need for a hydrogen precursor during the growth step. Moreover, any addition of hydrogen gas in the growth step results in defective graphene on copper films, which can be explained by excessive hydrogen resulting in the undesired etching of graphene,[17,28] evidenced by a rise in the D-peak (Figure 3 and Supporting Information, Figure S7).

The commensurate growth of graphene on evaporated copper is facilitated by the close lattice match between hexagonal graphene (lattice constant 2.46 Å at 300 °C) and hexagonal (111) Cu (lattice constant 2.56 Å at 300 °C).[14,19] Scanning electron microscope (SEM) inspection of incomplete graphene monolayer synthesis (Figure 4c) points to the nucleation of graphene on growing copper domains. Subsequently, graphene domains commensurately expand in size as the copper domains grow larger, reaching a domain size of *ca.* 20–40 μm for 5–10 min growth. Unlike prior CVD growth of graphene on heteroepitaxial cobalt, nickel, and ruthenium films on crystalline substrates,[29–31] the Raman spectroscopy of samples presented here show much weaker or negligible D-peak intensity, indicating higher quality monolayer graphene. The results here are comparable, but with cost and scale advantages, to those achieved with epitaxial copper on expensive sapphire substrates.[14] Likewise, commensurate growth on copper films on scalable silicon substrates promises substantial industrial advantages, compared to growth on expensive single-crystal Cu (111), Ni (111), Ru (0001), and Ir (111) metal substrates.[14,19,32–37] The Raman signatures of the observed graphene growth are compared to other reported CVD graphene on copper films in Table 1, and to various sources of graphene[14,19,29–41] (see Table S1 in the Supporting Information).

CONCLUSIONS

Our investigation demonstrates that monolayer graphene can be grown on evaporated copper films over a wide temperature range (875–1000 °C) with negligible defects in a hydrogen-free methane precursor. In addition, the graphene grains are correlated with the copper grains, affording a potential pathway for increasing the graphene grain size *via* control of the copper grains. Moreover, evaporated copper film, compared to expensive single crystal metal catalysts, is a promising avenue for graphene synthesis that can be directly integrated into standard device manufacturing in a cost-effective and scalable manner. Our findings also raised fundamental questions about differences in the CVD growth of graphene on copper film *versus* foil. The high-quality monolayer graphene obtained in this work was likely enabled by the distinct properties of hydrogen-rich (111) copper films as indicated by X-ray diffraction and TOF-SIMS. Future systematic studies on the growth characteristics of graphene on copper films are expected to enable further improvement in monolayer quality and grain size.

MATERIALS AND METHODS

Graphene synthesis: Chemical vapor deposition of graphene in this study was carried out in a vertical cold-wall chamber with independent control of temperature through showerhead and substrate heaters. The sample was initially heated to 600 °C at a ramp rate of 200 °C/min, and subsequently to the desired temperature for annealing and reduction of the copper surface at a ramp rate of 50 °C/min. This annealing step was done in a hydrogen environment for 5 min at the same temperature as the subsequent growth step. Ultrahigh purity methane (99.999% from Matheson) with typical flow rates of 5–10 sccm was circulated for 5 min for graphene synthesis. After growth, the chamber was cooled from the growth temperature to 550 °C at a rate of 50 °C/min in a gas-free chamber. The heaters were then turned off and cooling continued with 500 sccm of flowing N_2 gas. Samples were removed from the CVD chamber at temperatures below 180 °C. In each batch of CVD, e-beam evaporated copper film and commercial copper foil (Alfa Aesar stock no. 13382) were present for the comparison of growth results.

Material characterization: Renishaw In-Via Raman Microscope with He–Cd blue laser (442 nm wavelength) was employed for the Raman spectroscopy of graphene samples. A Zeiss Neon 40 scanning electron microscope and Veeco tapping-mode atomic

force microscope were used for morphology and surface analysis. Electron back scattering diffraction (EBSD) was performed on an EDAX/TSL OIM collection system attached to the aforementioned SEM and analyzed with MATLAB for digitized inversed pole figure. X-ray diffraction was performed on a Philips X'Pert Pro X-ray system, and depth profiling of hydrogen was carried out on an IONTOF GmbH time-of-flight secondary ion mass spectroscope with 1 nm depth resolution.

Conflict of Interest: The authors declare no competing financial interest.

Acknowledgment. The authors thank A. Lee, K. N. Parrish, Dr. Y. Hao, and Dr. H. Li for insightful discussions. Graphene synthesis was performed in an Aixtron Black Magic system. The experimental work has been carried out at the National Nanotechnology Infrastructure Network (NNIN) and Texas Materials Institute (TMI) facilities at The University of Texas at Austin. We appreciate Y. Wang and Prof. Paul Ho for their assistance with the EBSD facility as well as Matias Babenco for imaging analysis with MATLAB. This work is supported in part by the Nanoelectronic Research Initiative (NRI-SWAN Center), and the Office of Naval Research under the program of Dr. Chagaan Baatar.

Supporting Information Available: Figure S1−S7 as described in the main text. This material is available free of charge *via* the Internet at http://pubs.acs.org.

REFERENCES AND NOTES

1. Li, X.; Zhu, Y.; Cai, W.; Borysiak, M.; Han, B.; Chen, D.; Piner, R. D.; Colombo, L.; Ruoff, R. S. Transfer of Large-Area Graphene Films for High-Performance Transparent Conductive Electrodes. *Nano Lett.* **2009**, *9*, 4359–4363.
2. Li, X.; Magnuson, C. W.; Venugopal, A.; An, J.; Suk, J. W.; Han, B.; Borysiak, M.; Cai, W.; Velamakanni, A.; Zhu, Y.; *et al.* Graphene Films with Large Domain Size by a Two-Step Chemical Vapor Deposition Process. *Nano Lett.* **2010**, *10*, 4328–4334.
3. Li, X.; Magnuson, C. W.; Venugopal, A.; Tromp, R. M.; Hannon, J. B.; Vogel, E. M.; Colombo, L.; Ruoff, R. S. Large-Area Graphene Single Crystals Grown by Low-Pressure Chemical Vapor Deposition of Methane on Copper. *J. Am. Chem. Soc.* **2011**, *133*, 2816–2819.
4. Reina, A.; Jia, X.; Ho, J.; Nezich, D.; Son, H.; Bulovic, V.; Dresselhaus, M. S.; Kong, J. Large Area, Few-Layer Graphene Films on Arbitrary Substrates by Chemical Vapor Deposition. *Nano Lett.* **2008**, *9*, 30–35.
5. Schedin, F.; Geim, A. K.; Morozov, S. V.; Hill, E. W.; Blake, P.; Katsnelson, M. I.; Novoselov, K. S. Detection of Individual Gas Molecules Adsorbed on Graphene. *Nat. Mater.* **2007**, *6*, 652–655.
6. Balandin, A. A.; Ghosh, S.; Bao, W.; Calizo, I.; Teweldebrhan, D.; Miao, F.; Lau, C. N. Superior Thermal Conductivity of Single-Layer Graphene. *Nano Lett.* **2008**, *8*, 902–907.
7. Avouris, P.; Chen, Z.; Perebeinos, V. Carbon-Based Electronics. *Nat. Nanotechnol.* **2007**, *2*, 605–615.
8. Geim, A. K.; Novoselov, K. S. The Rise of Graphene. *Nat. Mater.* **2007**, *6*, 183–191.
9. Geim, A. K. Graphene: Status and Prospects. *Science* **2009**, *324*, 1530–1534.
10. Schwierz, F. Graphene Transistors. *Nat. Nanotechnol.* **2010**, *5*, 487–496.
11. Levendorf, M. P.; Ruiz-Vargas, C. S.; Garg, S.; Park, J. Transfer-Free Batch Fabrication of Single Layer Graphene Transistors. *Nano Lett.* **2009**, *9*, 4479–4483.
12. Lee, Y.; Bae, S.; Jang, H.; Jang, S.; Zhu, S.-E.; Sim, S. H.; Song, Y. I.; Hong, B. H.; Ahn, J.-H. Wafer-Scale Synthesis and Transfer of Graphene Films. *Nano Lett.* **2010**, *10*, 490–493.
13. Su, C. Y.; Lu, A. Y.; Wu, C. Y.; Li, Y. T.; Liu, K. K.; Zhang, W.; Lin, S. Y.; Juang, Z. Y.; Zhong, Y. L.; Chen, F. R.; *et al.* Direct Formation of Wafer Scale Graphene Thin Layers on Insulating Substrates by Chemical Vapor Deposition. *Nano Lett.* **2011**, *11*, 3612–3616.
14. Hu, B.; Ago, H.; Ito, Y.; Kawahara, K.; Tsuji, M.; Magome, E.; Sumitani, K.; Mizuta, N.; Ikeda, K.-i.; Mizuno, S. Epitaxial Growth of Large-Area Single-Layer Graphene over Cu(111)/Sapphire by Atmospheric Pressure CVD. *Carbon* **2012**, *50*, 57–65.
15. Ismach, A.; Druzgalski, C.; Penwell, S.; Schwartzberg, A.; Zheng, M.; Javey, A.; Bokor, J.; Zhang, Y. Direct Chemical Vapor Deposition of Graphene on Dielectric Surfaces. *Nano Lett.* **2010**, *10*, 1542–1548.
16. Lee, Y.-H.; Lee, J.-H. Scalable Growth of Free-Standing Graphene Wafers with Copper(Cu) Catalyst on SiO_2/Si Substrate: Thermal Conductivity of the Wafers. *Appl. Phys. Lett.* **2010**, *96*, 083101–083103.
17. Vlassiouk, I.; Regmi, M.; Fulvio, P.; Dai, S.; Datskos, P.; Eres, G.; Smirnov, S. Role of Hydrogen in Chemical Vapor Deposition Growth of Large Single-Crystal Graphene. *ACS Nano* **2011**, *5*, 6069–6076.
18. Cai, W. Large Area Few-Layer Graphene/Graphite Films as Transparent Thin Conducting Electrodes. *Appl. Phys. Lett.* **2009**, *95*, 123115.
19. Gao, L.; Guest, J. R.; Guisinger, N. P. Epitaxial Graphene on Cu(111). *Nano Lett.* **2010**, *10*, 3512–3516.
20. Mattevi, C.; Kim, H.; Chhowalla, M. A Review of Chemical Vapour Deposition of Graphene on Copper. *J. Mater. Chem.* **2011**, *21*, 3324–3334.
21. Nemes-Incze, P.; Yoo, K. J.; Tapasztó, L.; Dobrik, G.; Lábár, J.; Horváth, Z. E.; Hwang, C.; Biró, L. P. Revealing the Grain Structure of Graphene Grown by Chemical Vapor Deposition. *Appl. Phys. Lett.* **2011**, *99*, 023104.
22. Zhao, L.; Rim, K. T.; Zhou, H.; He, R.; Heinz, T. F.; Pinczuk, A.; Flynn, G. W.; Pasupathy, A. N. Influence of Copper Crystal Surface on the CVD Growth of Large Area Monolayer Graphene. *Solid State Commun.* **2011**, *151*, 509–513.
23. Wood, J. D.; Schmucker, S. W.; Lyons, A. S.; Pop, E.; Lyding, J. W. Effects of Polycrystalline Cu Substrate on Graphene Growth by Chemical Vapor Deposition. *Nano Lett.* **2011**, *11*, 4547–4554.
24. Bhaviripudi, S.; Jia, X.; Dresselhaus, M. S.; Kong, J. Role of Kinetic Factors in Chemical Vapor Deposition Synthesis of Uniform Large Area Graphene Using Copper Catalyst. *Nano Lett.* **2010**, *10*, 4128–4133.
25. Strömquist, J.; Bengtsson, L.; Persson, M.; Hammer, B. The Dynamics of H Absorption in and Adsorption on Cu(111). *Surf. Sci.* **1998**, *397*, 382–394.
26. Kammler, T.; Küppers, J. Interaction of H Atoms with Cu(111) Surfaces: Adsorption, Absorption, and Abstraction. *J. Chem. Phys.* **1999**, *111*, 8115–8123.
27. Thomsen, L.; Onsgaard, J.; Godowski, P. J.; Møller, P.; Hoffmann, S. V. Adsorption of Hydrogen on Clean and Potassium Modified Low Index Copper Surfaces: Cu(100) and Cu(110). *J. Vac. Sci. Technol., A* **2001**, *19*, 1988–1992.
28. Gao, L.; Ren, W.; Zhao, J.; Ma, L.-P.; Chen, Z.; Cheng, H.-M. Efficient Growth of High-Quality Graphene Films on Cu Foils by Ambient Pressure Chemical Vapor Deposition. *Appl. Phys. Lett.* **2010**, *97*, 183109.
29. Ago, H.; Ito, Y.; Mizuta, N.; Yoshida, K.; Hu, B.; Orofeo, C. M.; Tsuji, M.; Ikeda, K.-i.; Mizuno, S. Epitaxial Chemical Vapor Deposition Growth of Single-Layer Graphene over Cobalt Film Crystallized on Sapphire. *ACS Nano* **2010**, *4*, 7407–7414.
30. Iwasaki, T.; Park, H. J.; Konuma, M.; Lee, D. S.; Smet, J. H.; Starke, U. Long-Range Ordered Single-Crystal Graphene on High-Quality Heteroepitaxial Ni Thin Films Grown on Mgo(111). *Nano Lett.* **2010**, *11*, 79–84.
31. Sutter, P. W. Graphene Growth on Epitaxial Ru Thin Films on Sapphire. *Appl. Phys. Lett.* **2010**, *97*, 213101.
32. Gamo, Y.; Nagashima, A.; Wakabayashi, M.; Terai, M.; Oshima, C. Atomic Structure of Monolayer Graphite Formed on Ni(111). *Surf. Sci.* **1997**, *374*, 61–64.
33. N'Diaye, A. T.; Bleikamp, S.; Feibelman, P. J.; Michely, T. Two-Dimensional Ir Cluster Lattice on a Graphene Moiré on Ir(111). *Phys. Rev. Lett.* **2006**, *97*, 215501.
34. Marchini, S.; Günther, S.; Wintterlin, J. Scanning Tunneling Microscopy of Graphene on Ru(0001). *Phys. Rev. B* **2007**, *76*, 075429.

35. Sutter, P. W.; Flege, J.-I.; Sutter, E. A. Epitaxial Graphene on Ruthenium. *Nat. Mater.* **2008**, *7*, 406–411.
36. Usachov, D.; Dobrotvorskii, A. M.; Varykhalov, A.; Rader, O.; Gudat, W.; Shikin, A. M.; Adamchuk, V. K. Experimental and Theoretical Study of the Morphology of Commensurate and Incommensurate Graphene Layers on Ni Single-Crystal Surfaces. *Phys. Rev. B* **2008**, *78*, 085403.
37. Reddy, K. M. High Quality, Transferrable Graphene Grown on Single Crystal Cu(111) Thin Films on Basal-Plane Sapphire. *Appl. Phys. Lett.* **2011**, *98*, 113117.
38. Emtsev, K. V.; Bostwick, A.; Horn, K.; Jobst, J.; Kellogg, G. L.; Ley, L.; McChesney, J. L.; Ohta, T.; Reshanov, S. A.; Rohrl, J.; *et al*. Towards Wafer-Size Graphene Layers by Atmospheric Pressure Graphitization of Silicon Carbide. *Nat. Mater.* **2009**, *8*, 203–207.
39. Robinson, J. A.; Wetherington, M.; Tedesco, J. L.; Campbell, P. M.; Weng, X.; Stitt, J.; Fanton, M. A.; Frantz, E.; Snyder, D.; VanMil, B. L.; *et al.* Correlating Raman Spectral Signatures with Carrier Mobility in Epitaxial Graphene: A Guide to Achieving High Mobility on the Wafer Scale. *Nano Lett.* **2009**, *9*, 2873–2876.
40. Ferrari, A. C.; Meyer, J. C.; Scardaci, V.; Casiraghi, C.; Lazzeri, M.; Mauri, F.; Piscanec, S.; Jiang, D.; Novoselov, K. S.; Roth, S.; *et al*. Raman Spectrum of Graphene and Graphene Layers. *Phys. Rev. Lett.* **2006**, *97*, 187401.
41. Graf, D.; Molitor, F.; Ensslin, K.; Stampfer, C.; Jungen, A.; Hierold, C.; Wirtz, L. Spatially Resolved Raman Spectroscopy of Single- and Few-Layer Graphene. *Nano Lett.* **2007**, *7*, 238–242.